The Canadian Mineralogist
Vol. 45, pp. 935-943 (2007)
DOI: 10.2113/gscanmin.45.4.935

THE CRYSTAL STRUCTURE OF KAMPFITE

Laurel C. BASCIANO[§] and Lee A. GROAT[¶]

Department of Earth and Ocean Sciences, University of British Columbia, Vancouver, British Columbia V6T 1Z4, Canada

Abstract

The crystal structure of kampfite, ideally $Ba_{12}(Si_{11}Al_5)O_{31}(CO_3)_8Cl_5$, *a* 31.2329(7), *b* 5.2398(1), *c* 9.0966(3) Å, β 106.933(2)°, *V* 1424.2(1) Å^3, *Cc*, *Z* = 1, has been solved by direct methods and refined to an *R* index of 2.3% for 2938 observed ($|F_o| > 4\sigma F$) reflections collected with a four-circle diffractometer using Mo*K*α radiation and a CCD detector. The kampfite structure is based on double layers of tetrahedra, $[T_4O_8]$, consisting of six-membered rings oriented parallel to (100). The layers of tetrahedra are connected by slabs of Ba polyhedra composed of a layer of BaO_6Cl_6 polyhedra, with all of the Ba and Cl atoms sharing a common plane parallel to (100), flanked on either side by a layer of BaO_9Cl polyhedra. The CO_3 groups lie between the layers of Ba polyhedra and are oriented approximately parallel to (100). The layering of TO_4 tetrahedra and Ba polyhedra is responsible for the perfect {100} cleavage of kampfite. Kampfite is part of the monteregianite-(Y) – wickenburgite series and is structurally and chemically similar to cymrite.

Keywords: kampfite, crystal structure, chemical formula, barium mineral.

Sommaire

Nous avons résolu la structure cristalline de la kampfite, de composition idéale $Ba_{12}(Si_{11}Al_5)O_{31}(CO_3)_8Cl_5$, *a* 31.2329(7), *b* 5.2398(1), *c* 9.0966(3) Å, β 106.933(2)°, *V* 1424.2(1) Å^3, *Cc*, *Z* = 1, par méthodes directes, et nous l'avons affiné jusqu'à un résidu *R* de 2.3% pour 2938 réflexions observées ($|F_o| > 4\sigma F$) prélevées avec rayonnement Mo*K*α et un diffractomètre à quatres cercles muni d'un détecteur CCD. La structure contient des couches doubles de tétraèdres, $[T_4O_8]$, agencés en anneaux de six tétraèdres orientés parallèle à (100). Les couches de tétraèdres sont interconnectées par des plaquettes de polyèdres BaO_6Cl_6 ayant tous les atomes alignés sur un plan parallèle à (100), flanquées de chaque côté par des couches de polyèdres BaO_9Cl. Les groupes CO_3 sont disposés entre les couches de polyèdres Ba et orientés à peu près parallèles à (100). La stratification des tétraèdres TO_4 et des polyèdres Ba rend compte du clivage {100} parfait. La kampfite fait partie de la série montérégianite-(Y) – wickenburgite, et serait semblable à la cymrite des points de vues structuraux et chimiques.

(Traduit par la Rédaction)

Mots-clés: kampfite, structure cristalline, formule chimique, minéral de barium.

Introduction

Kampfite was first described by Basciano *et al*. (2001). The single crystal used for the X-ray-diffraction studies was reported to be uniaxial negative, with indices of refraction ω 1.642 ± 0.002 and ε 1.594 Å 0.002 (measured at 589 nm). Application of the Gladstone–Dale relationship (Mandarino 1981) gave a compatibility index of –0.059 (fair). However, another grain was described as biaxial negative with $2V_{meas}$ of 20(5)° and indices of refraction α 1.641 ± 0.001, β 1.642 ± 0.001, γ_{calc} 1.642, slight dispersion, $r < v$. The ideal formula for kampfite (based on electron-microprobe data and the results of the crystal-structure study) was given as $Ba_6[(Si,Al)O_2]_8(CO_3)_2Cl_2(Cl,H_2O)_2$. Micro-infrared absorption spectroscopy suggested the presence of both CO_3 and H_2O. Precession single-crystal photographs suggested to Basciano *et al*. (2001) that kampfite is hexagonal, with approximate unit-cell dimensions *a* 5.25, *c* 29.8 Å, and the possible space-groups were reported as $P6_3/mmc$, $P\bar{6}2c$, $P6_3mc$, $P\bar{3}1c$, and $P31c$. The structure was solved and refined in each of the space groups indicated as being compatible with the precession single-crystal photographs, and the best

§ *Present address*: Department of Geological Sciences and Geological Engineering, Queen's University, Kingston, Ontario K7L 3N6, Canada.
¶ *E-mail address*: lgroat@eos.ubc.ca

results ($R_1 \approx 5\%$) were obtained for space group $P6_3mc$. However, the bond lengths reported differed seriously from expected values and lacked internal consistency (Basciano *et al.* 2001); for example, the *T*–O distances ranged from 1.53 to 1.80 Å. Careful inspection of the crystal used under a polarizing microscope showed that it is likely composed of two individuals, and this was given as the most probable reason for the poor quality of the data.

Subsequently, several crystals were studied optically, and all were found to be biaxial, which casts doubt on the original optical work. In order to resolve ambiguities concerning the symmetry and crystal structure of kampfite, we decided to collect X-ray data from a different single crystal. We report here information derived from the superior dataset.

Chemical Composition

Chemical analyses were performed with a Cameca SX100 electron microprobe at the University of Manitoba, operating in the wavelength-dispersion mode at the following conditions: excitation voltage 15 kV, beam current 20 nA, and beam diameter 10 μm. The following standards were used: albite (Na*K*α), andalusite (Al*K*α), diopside (Si*K*α), tugtupite (Cl*K*α), titanite (Ti*K*α), strontianite (Sr*K*α), and barite (Ba*L*α). Rare-earth elements and Pb were sought but not detected. Micro infrared-absorption spectroscopy of a cleavage fragment with no visible inclusions showed no indication of structural H_2O, contrary to the results of Basciano *et al.* (2001), which we assume to have resulted from hydrous inclusions. The results of the electron-microprobe study are given in Table 1. On the basis of 16 *T* (Si^{4+} + Ti^{4+} + Al^{3+}) and 8 C cations per formula unit (*pfu*), as derived from the crystal-structure study, the following empirical formula was calculated from an average result of 10 analyses of the crystal used for structure work: $(Ba_{12.13}Na_{0.06}Sr_{0.03})_{\Sigma 12.21}(Si_{10.77}Al_{5.18}Ti_{0.05})_{\Sigma 16.00}C_{8.00}O_{55.14}Cl_{4.93}$. The calculated density based on these data (and the unit-cell parameters from the crystal-structure study) is 3.809 g/cm^3, and application of the Gladstone–Dale relationship (Mandarino 1981) with the biaxial optical data given above results in a compatibility index of –0.015 (superior). As shown in Table 1, the chemical composition presented in Basciano *et al.* (2001), which was obtained from a different sample using a JEOL 733 electron microprobe at the Canadian Museum of Nature, is very similar.

TABLE 1. CHEMICAL COMPOSITION OF KAMPFITE

	Basciano *et al.* (2001)	Structure crystal	Standard deviation	Range
n	3	10		
CO_2* wt.%	10.73	10.74	-	-
SiO_2	20.14	19.75	0.12	19.54-19.95
TiO_2	b.d.l.	0.11	0.04	0.03-0.16
Al_2O_3	7.76	8.06	0.06	7.98-8.16
CaO	0.06	b.d.l.	-	-
SrO	b.d.l.	0.10	0.03	0.06-0.15
BaO	57.72	56.74	0.21	56.43-57.11
Na_2O	0.08	0.06	0.02	0.02-0.09
Cl	5.60	5.33	0.02	5.29-5.37
O=Cl	-1.26	-1.20		
Total	100.82	99.69		
C *apfu*	8.00	8.00		
Si	11.00	10.77		
Ti	-	0.05		
Al	5.00	5.18		
Ca	0.04	-		
Sr	-	0.03		
Ba	12.36	12.13		
Na	0.09	0.06		
Cl	5.19	4.93		
O	55.34	55.14		

Note: Compositions were recalculated on the basis of 16 (Si + Ti + Al) atoms per unit cell. *n* = number of points. * Determined by stoichiometry. b.d.l.: below detection limit.

X-Ray-Diffraction Experiment

The crystal used in this study is from the Esquire #1 claim at Rush Creek, Fresno County, California. An inclusion-free cleavage fragment was selected for the structure analysis. Subsequent to the collection of structure data (below), powder-diffraction data were collected with a Bruker D8 Discover/GADDS instrument at the Canadian Museum of Nature. The results (Table 2) agree well with those reported in Basciano *et al.* (2001), although six of the 45 reflections (two with $I_{est} \approx 15$) reported in the earlier study were not seen in the new data. It was not possible to refine the monoclinic unit-cell because of peak overlap.

Crystal-structure data were collected with a Bruker single-crystal diffractometer with a charge-coupled device (CCD) area detector and Mo*K*α radiation (experimental details are given in Table 3). Intensity data were collected to 60° 2θ using a frame width of 0.1° and a frame time of 30 s. Frame sequences uniformly distributed through the entire dataset were sampled to give intense reflections for least-squares refinement of the cell parameters and orientation matrix. The initial reduced primitive cell with *a* 5.240, *b* 9.097, *c* 15.835 Å, α 73.31, β 80.48, γ 90.00°, was transformed to a metrically orthogonal *I*-centered cell [$\bar{1}$ 0 0 / 0 $\bar{1}$ 0 / $\bar{1}$ $\bar{1}$ 2], and the resulting orientation-matrix was then used for three-dimensional integration of the intensity data. Standard corrections (for Lorentz, polarization, and background effects) were applied. The reflections were indexed with the following unit-cell parameters, based on least-squares refinement of 6108 reflections with $I > 10\sigma I$ and a triclinic metric constraint: *a* 5.2398(1), *b* 9.0966(2), *c* 29.8789(7) Å, α 90.005(2), β 89.997(2), γ 90.001(2)°, V = 1424.2(1) Å^3. The absorption was corrected using an empirical plate shape (001) with a glancing angle of 3°. Of the 12,166 reflections collected, 11,165 remained after rejection of those within the glancing angle. Identical reflections (at different Ψ

angles) were combined to give a total of 6962 reflections in the Ewald sphere.

The orthogonal *I*-centered cell has twice the volume of the earlier reported hexagonal cell (Basciano *et al.* 2001); however, the two cells are not simply related. The hexagonal cell with a = 5.25, c = 29.8 Å, when doubled in volume *via* [0 1 0 / $\bar{2}$ $\bar{1}$ 0 / 0 0 1], produces an orthogonal cell of similar size. It is *C*-centered rather than *I*-centered, however. To fully test for the *I*-centering, the data frames were re-integrated without an imposed lattice constraint; the resulting systematically absent reflections clearly support *I*-centering and *Iba** diffraction symmetry, consistent with orthorhombic space-groups *Ibam* and *Iba*2. The structure is clearly acentric, suggesting *Iba*2; however, the *a*-glide perpendicular to *b* and the two-fold rotational axis along *c* are inconsistent with some of the structural elements. Although the intensities merge well in orthorhombic symmetry (R_{merge} = 3.4%), the overall structure is inconsistent with the orthorhombic system. Possible monoclinic space-groups are *Ib*-- and *I*2-, with R_{merge} values of 2.8 and 2.7%, respectively. In *Ib*, of the 3950 unique data, 2938 were observed ($F_o > 4\sigma F$).

Structure Solution and Refinement

Scattering factors for neutral atoms, together with anomalous dispersion corrections, were taken from the *International Tables for Crystallography* (1992). The Bruker SHELXTL Version 5 system of programs was used for solution and refinement of the crystal structure. The structure was solved in *I*1 using direct methods and, after analysis with MISSYM (LePage 1987), was re-refined in *Ib* and *I*2. The *I*1, *Ib*, and *I*2 refinements are fundamentally equivalent. Only the highest-symmetry model in *Ib* could be refined satisfactorily without constraining highly correlated refining parameters, however. Finally, the *Ib* model (unique axis **a**) was transformed to a more conventional monoclinic setting in *Cc* (unique axis **b**). The *Cc* model is fully anisotropic and converges well with refined occupancies and displacement parameters; final *R*-values are R_1 = 2.3% and wR_2 = 5.6% (refinements on F^2). It includes a minor extinction correction [0.00017(4)], and has a well-established absolute structural configuration [Flack index = 0.06(2)]. The only user-defined constraints are relatively minor: the occupancies of the two *C* sites refined to approximately the same value, so are constrained to be equivalent, as are the occupancies of the coordinating O positions. The largest correlation-matrix elements involve displacement parameters for the atoms at *Ba*(1) and *Ba*(2) (0.94 for U_{23} and 0.93 for U_{12}), and *Ba*(3) and *Cl*(2) (–0.93 for U_{23} and –0.91 for U_{12}). The next largest involve *y* for *Ba*(1) and *Ba*(2) (–0.91), O(6) and O(12) (0.86), *Ba*(3) and Cl(2) (0.84), and O(2) and O(9) (0.84). These are followed by *x* for Cl(1) and Cl(2) (0.80), U_{22} for O(13) and O(14) (–0.77), and the occupancies for *Ba*(3) and Cl(2) (–0.77). Final parameters of the atoms are listed in Table 4, selected interatomic distances and angles in Table 5, and bond valences in Table 6. Observed and calculated structure-factors may be obtained from The Depository of Unpublished Data on the MAC web site [document Kampfite (CM45_935)].

Description of the Structure

There are nine distinct cation sites in the kampfite structure; all are at general positions, and three contain Ba, four contain Si, Al, and minor Ti, and two contain

TABLE 2. X-RAY POWDER-DIFFRACTION DATA FOR KAMPFITE

d_{meas} (Å)	I_{meas}	d_{calc} (Å)	I_{calc}	*hkl*
14.883	46	14.94	100	200
4.547	10	4.549	6	$30\bar{2}$
		4.541	6	$11\bar{1}$, $1\bar{1}\bar{1}$
4.348	18	4.344	7	$1\bar{1}1$, 111, $31\bar{1}$, $3\bar{1}\bar{1}$
3.879	100	3.885	39	202, $60\bar{2}$
		3.880	39	$3\bar{1}1$, 311, $5\bar{1}\bar{1}$, $51\bar{1}$
3.717	5	3.735	2	800
3.355	31	3.358	17	402, $80\bar{2}$
		3.355	16	$5\bar{1}1$, 511, $7\bar{1}\bar{1}$, $71\bar{1}$
2.985	15	2.988	50	1000
2.883	27	2.887	16	602, $100\bar{2}$
		2.884	15	$7\bar{1}1$, 711, $9\bar{1}\bar{1}$, $91\bar{1}$
2.621	63	2.625	42	$31\bar{3}$, $3\bar{1}\bar{3}$
		2.620	48	020
2.584	8	2.585	3	$11\bar{3}$, $1\bar{1}\bar{3}$, $51\bar{3}$, $5\bar{1}\bar{3}$
		2.581	3	220, $22\bar{0}$
2.493	12	2.497	5	802, $120\bar{2}$
		2.496	6	$9\bar{1}1$, 911, $11\bar{1}\bar{1}$, $111\bar{1}$
2.270	10	2.274	9	$40\bar{4}$
		2.270	9	$22\bar{2}$, $2\bar{2}\bar{2}$
2.173	20	2.176	11	004, $80\bar{4}$
		2.172	10	$2\bar{2}2$, 222, $6\bar{2}\bar{2}$, $62\bar{2}$
2.146	10	2.147	7	$5\bar{1}3$, 513, $11\bar{1}\bar{3}$, $1\bar{1}\bar{1}\bar{3}$
		2.145	6	$8\bar{2}0$, 820
2.066	7	2.069	4	204, $100\bar{4}$
		2.066	4	$4\bar{2}2$, 422, $82\bar{2}$, $8\bar{2}\bar{2}$
1.970	21	1.972	14	$7\bar{1}3$, 713, $13\bar{1}\bar{3}$, $1\bar{3}\bar{1}\bar{3}$
		1.970	13	$10\bar{2}0$, $10\bar{2}0$
1.931	7	1.932	5	$12\bar{0}2$, $16\bar{0}2$, $13\bar{1}1$, 1311, $15\bar{1}\bar{1}$, $151\bar{1}$
1.673	9	1.674	3	$02\bar{4}$, 024, $82\bar{4}$, $8\bar{2}\bar{4}$
		1.672	3	$3\bar{3}1$, 331, $53\bar{1}$, $5\bar{3}\bar{1}$
1.622	3	1.622	2	$53\bar{1}$, 531, $7\bar{3}\bar{1}$, $73\bar{1}$
1.557	6	1.556	2	$10\bar{0}4$, $18\bar{0}4$
1.514	3	1.516	8	$60\bar{6}$
		1.514	6	$33\bar{3}$, $3\bar{3}\bar{3}$
1.488	1	1.488	1	931, 931, $11\bar{3}\bar{1}$, $113\bar{1}$
1.402	2	1.402	2	$18\bar{2}0$, $18\bar{2}0$
1.350	1	1.350	3	$7\bar{3}3$, 733, $13\bar{3}\bar{3}$, $133\bar{3}$
1.337	2	1.337	1	$13\bar{3}1$, 1331, $15\bar{3}\bar{1}$, $153\bar{1}$
1.311	1	1.312	5	$62\bar{6}$, $6\bar{2}\bar{6}$

TABLE 3. KAMPFITE: DATA COLLECTION AND STRUCTURE-REFINEMENT INFORMATION

a (Å)	31.2329(7)	Total F_o	12166
b (Å)	5.2398(1)	Unique F_o	6962
c (Å)	9.0966(3)	$F_o > 4\sigma F_o$	2938
β (°)	106.933(2)	R_{int} (%)	2.8(3)
V (Å^3)	1424.2(1)	Least-squares parameters	231
Space group	*Cc*	R_1 for $F_o > 4\sigma F_o$ (%)	2.3
Z	1	R_1 for all unique F_o (%)	3.7
Crystal size (mm)	0.2 × 0.2 × 0.013	wR_2 (%)	5.6
Radiation	MoKα	a	0.0329
Monochromator	graphite	b	0.0
		GooF (= *S*)	0.943

Note: $w = 1/[\sigma^2(F_o^2) + (a \times P)^2 + b \times P]$, where $P = [\text{Max}(F_o^2, 0) + 2 \times F_c^2)]/3$.

TABLE 4. FINAL ATOM-PARAMETERS FOR KAMPFITE

	x	*y*	*z*	e	U_{11}	U_{22}	U_{33}	U_{12}	U_{13}	U_{23}	U_{eq}
Ba(1)	0.39588(1)	0.2498(2)	0.05925(3)	56	0.0175(2)	0.0197(2)	0.0151(2)	-0.0014(3)	0.0047(1)	0.0014(3)	0.01741(9)
Ba(2)	0.61035(1)	0.2503(2)	0.27376(3)	56	0.0172(2)	0.0196(2)	0.0154(2)	-0.0012(3)	0.0052(1)	-0.0022(3)	0.01730(9)
Ba(3)	0.00309(2)	0.2503(2)	0.33408(6)	51.1(2)	0.0157(2)	0.0166(2)	0.0160(2)	0.0005(3)	0.0047(1)	-0.0001(3)	0.0161(1)
T(1)	0.19850(7)	0.1885(4)	0.5271(2)	14	0.014(1)	0.015(1)	0.011(1)	-0.0013(7)	0.0001(9)	-0.0004(6)	0.0142(5)
T(2)	0.19884(8)	0.3121(3)	0.1973(3)	14	0.0138(9)	0.0128(9)	0.0125(8)	0.0017(9)	0.0037(7)	-0.0003(7)	0.0131(4)
T(3)	0.30741(8)	0.3118(3)	0.3059(3)	14	0.0138(9)	0.0110(9)	0.0125(8)	0.0000(9)	0.0054(7)	0.0001(7)	0.0121(4)
T(4)	0.30768(7)	0.1888(4)	0.6361(2)	14	0.013(1)	0.012(1)	0.013(1)	-0.0003(6)	0.006(1)	0.0008(5)	0.0123(5)
C(1)	0.0736(2)	0.2483(8)	0.0693(5)	7.98(9)	0.019(2)	0.021(2)	0.019(2)	-0.001(2)	0.007(1)	0.000(2)	0.020(1)
C(2)	0.4327(2)	0.2461(8)	0.4289(5)	7.98(9)	0.018(2)	0.021(2)	0.017(2)	0.000(2)	0.005(1)	0.003(2)	0.0190(9)
O(1)	0.4299(2)	0.033(1)	0.3556(9)	6.71(4)	0.020(3)	0.022(3)	0.021(3)	0.007(2)	0.010(2)	0.002(2)	0.020(1)
O(2)	0.4320(2)	0.255(2)	0.5724(5)	6.71(4)	0.025(2)	0.023(2)	0.018(2)	-0.001(2)	0.001(2)	0.008(3)	0.023(1)
O(3)	0.4307(3)	0.464(1)	0.3545(9)	6.71(4)	0.019(3)	0.033(4)	0.022(3)	0.007(3)	0.009(2)	-0.002(3)	0.024(2)
O(4)	0.3272(2)	0.5988(9)	0.2758(5)	8	0.019(2)	0.016(2)	0.017(2)	-0.002(2)	0.004(2)	0.000(2)	0.0175(9)
O(5)	0.3266(2)	0.0982(9)	0.2031(5)	8	0.015(2)	0.016(2)	0.019(2)	-0.002(2)	0.008(2)	-0.002(2)	0.0165(9)
O(6)	0.3288(1)	0.232(1)	0.4907(5)	8	0.017(2)	0.031(3)	0.015(2)	0.006(3)	0.008(2)	0.007(2)	0.020(1)
O(7)	0.0763(3)	0.028(1)	0.002(9)	6.71(4)	0.023(3)	0.026(3)	0.021(3)	-0.007(2)	0.003(2)	0.004(2)	0.024(2)
O(8)	0.0757(2)	0.461(1)	-0.0003(9)	6.71(4)	0.021(3)	0.017(3)	0.024(3)	-0.003(2)	0.009(2)	-0.001(2)	0.020(1)
O(9)	0.0741(2)	0.257(2)	0.2136(6)	6.71(4)	0.024(2)	0.023(2)	0.024(2)	0.001(2)	0.009(2)	0.008(3)	0.023(1)
O(10)	0.1797(2)	0.0987(9)	0.0574(5)	8	0.020(2)	0.014(2)	0.017(2)	-0.002(2)	0.001(2)	0.000(2)	0.0177(9)
O(11)	0.1793(2)	0.5999(9)	0.1262(6)	8	0.022(2)	0.011(2)	0.023(2)	0.001(2)	0.009(2)	0.000(2)	0.0184(9)
O(12)	0.1776(2)	0.232(1)	0.3395(5)	8	0.020(2)	0.027(3)	0.018(2)	-0.008(3)	0.003(2)	0.001(2)	0.022(1)
O(13)	0.2532(2)	0.1957(7)	0.5784(6)	8	0.016(2)	0.019(2)	0.017(2)	0.000(2)	0.004(1)	-0.007(2)	0.0178(9)
O(14)	0.2532(2)	0.3114(7)	0.2557(7)	8	0.011(2)	0.021(2)	0.018(2)	0.001(2)	0.003(1)	0.006(2)	0.0167(9)
Cl(1)	0.5031(1)	0.2499(2)	0.1675(3)	17	0.0209(5)	0.0201(5)	0.0183(5)	-0.008(2)	0.0055(4)	-0.004(2)	0.0198(2)
Cl(2)	0.5030(6)	0.255(3)	0.500(1)	4.1(2)	0.049(5)	0.019(3)	0.007(3)	0.009(5)	0.012(3)	0.006(5)	0.024(2)

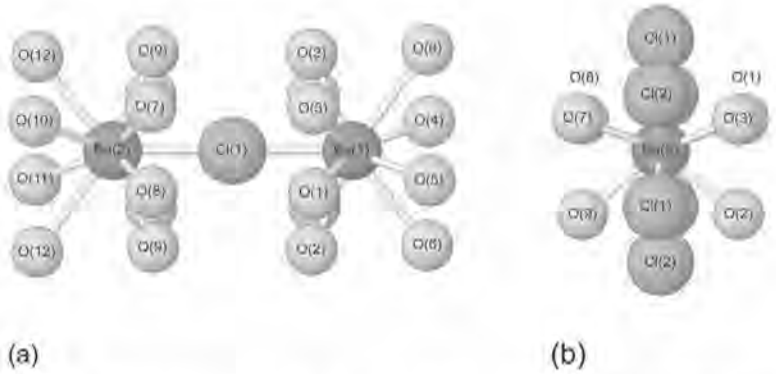

FIG. 1. (a) Coordination of *Ba*(1) and *Ba*(2) in kampfite (projected along [001] with [010] vertical). (b) Coordination of *Ba*(3) in kampfite (projected approximately along [010] with [001] vertical). In both diagrams, the partially hidden atoms have the same labels as those in front of them, except for O(1) and O(8).

C. The atom at the *Ba*(1) site is coordinated by 11 anions (ten O and one Cl; Fig. 1a). The Ba(1)–ϕ (ϕ: O, Cl) distances range from 2.810 to 3.377 Å (mean 2.971 Å). The electron-microprobe data, refined site-occupancy, and bond-valence analysis (Table 6) suggest that *Ba*(1) is completely filled with Ba.

The atom at the *Ba*(2) site is also coordinated by 11 anions (ten O and one Cl; Fig. 1a). The Ba(2)–ϕ distances range from 2.798 to 3.380 Å (mean 2.974 Å). The chemical data, refined site-occupancy, and bond-valence analysis suggest that *Ba*(2) is completely filled with Ba.

TABLE 5. SELECTED INTERATOMIC DISTANCES (Å) AND ANGLES (°) FOR KAMPFITE

Ba(1)–O(1)*a*	2.810(8)	*T*(1)–O(13)	1.636(7)	O(13)–*T*(1)–O(11)*i*	110.2(3)
–O(2)*b*	2.819(9)	–O(11)*i*	1.649(5)	–O(12)	110.9(3)
–O(3)	2.820(8)	–O(12)	1.656(5)	–O(10)*h*	111.2(3)
–O(1)	2.832(8)	–O(10)*h*	1.667(5)	O(11)*i*–*T*(1)–O(12)	112.0(3)
–O(3)*b*	2.843(8)	<*T*(1)–O>	1.652	–O(10)*h*	108.4(3)
–O(2)*a*	2.864(8)			O(12)–*T*(1)–O(10)*h*	104.0(3)
–O(4)*b*	2.943(5)	*T*(2)–O(14)	1.624(6)	<O–*T*(1)–O>	109.5
–O(5)	2.945(5)	–O(10)	1.668(5)		
–Cl(1)	3.203(3)	–O(12)	1.671(5)	O(14)–*T*(2)–O(10)	110.8(3)
–O(6)*a*	3.224(6)	–O(11)	1.684(5)	–O(12)	111.1(3)
–O(6)*b*	3.377(7)	<*T*(2)–O>	1.662	–O(11)	110.8(3)
<*Ba*(1)–ϕ>	2.971			O(10)–*T*(2)–O(12)	106.7(3)
		T(3)–O(14)	1.621(6)	–O(11)	107.3(3)
Ba(2)–O(7)*c*	2.798(8)	–O(6)	1.671(5)	O(12)–*T*(2)–O(11)	110.0(3)
–O(8)*d*	2.814(8)	–O(5)	1.678(5)	<O–*T*(2)–O>	109.5
–O(9)*e*	2.813(9)	–O(4)	1.679(5)		
–O(7)*d*	2.843(8)	<*T*(3)–O>	1.662	O(14)–*T*(3)–O(6)	111.2(3)
–O(8)*e*	2.848(8)			–O(5)	110.9(3)
–O(9)*c*	2.874(8)	*T*(4)–O(13)	1.628(6)	–O(4)	111.1(3)
–O(10)*d*	2.954(5)	–O(6)	1.655(5)	O(6)–*T*(3)–O(5)	106.9(3)
–O(11)*e*	2.956(5)	–O(5)h	1.665(5)	–O(4)	109.3(3)
–Cl(1)	3.205(3)	–O(4)i	1.665(5)	O(5)–*T*(3)–O(4)	107.4(3)
–O(12)*c*	3.224(6)	<*T*(4)–O>	1.653	<O–*T*(3)–O>	109.5
–O(12)*e*	3.380(7)				
<*Ba*(2)–ϕ>	2.974	*C*(1)–O(8)	1.293(7)	O(13)–*T*(4)–O(6)	111.1(3)
		–O(9)	1.308(7)	–O(5)	111.4(3)
Ba(3)–O2*f*	2.741(5)	–O(7)	1.320(8)	–O(4)	110.3(3)
–O(9)	2.745(5)	<*C*(1)–O>	1.307	O(6)–*T*(4)–O(5)	103.5(3)
–O(3)*g*	2.765(8)			–O(4)	112.1(3)
–O(7)*h*	2.767(7)	*C*(2)–O(1)	1.291(7)	O(5)–*T*(4)–O(4)	108.2(2)
–O(8)*i*	2.776(7)	–O(2)	1.312(7)	<O–*T*(4)–O>	109.4
–O(1)*j*	2.778(6)	–O(3)	1.319(7)		
–Cl(2)*g*	3.00(1)	<*C*(2)–O>	1.307	O(8)–*C*(1)–O(9)	118.3(6)
–Cl(1)*j*	3.025(2)			–O(7)	120.5(4)
–Cl(1)*g*	3.029(2)			O(9)–*C*(1)–O(7)	120.7(6)
–Cl(1)*k*	3.033(2)			<O–*C*(1)–O>	119.8
–Cl(2)*f*	3.039(9)				
–Cl(2)*j*	3.04(1)			O(1)–*C*(2)–O(2)	121.7(6)
<*Ba*(3)–ϕ>	2.90			–O(3)	119.9(4)
				O(2)–*C*(2)–O(3)	117.9(6)
				<O–*C*(2)–O>	119.8

Note: <*M*–ϕ> denotes the mean metal–ligand distance (Å). Equivalent positions: *a* = *x*, $\bar{y}$, *z* – ½; *b* = *x*, $\bar{y}$ + 1, *z* – ½; *c* = *x* + ½, *y* + ½, *z*; *d* = *x* + ½, $\bar{y}$ + ½, *z* + ½; *e* = *x* + ½, *y* – ½, *z*; *f* = *x* – ½, $\bar{y}$ + ½, *z* – ½; *g* = *x* – ½, *y* – ½, *z*; *h* = *x*, $\bar{y}$, *z* + ½; *i* = *x*, $\bar{y}$ + 1, *z* + ½; *j* = *x* – ½, *y* + ½, *z*; *k* = *x* – ½, $\bar{y}$ + ½, *z* + ½.

The atom at the *Ba*(3) site is coordinated by 12 anions (six O and six Cl; Fig. 1b). The Ba(3)–ϕ (ϕ: O, Cl) distances range from 2.741 to 3.04 Å (mean 2.90 Å). The electron-microprobe analyses suggest that the *Ba*(3) site is completely filled with Ba, but the refined site-occupancy indicates that approximately 8% of the *Ba*(3) sites are vacant. The difference-Fourier map shows no evidence of splitting of the *Ba*(3) site. The trace amounts of Sr and Na in the electron-microprobe data (and Ca in the data from Basciano *et al*. 2001) are most likely ordered at *Ba*(3). The bond-valence sum, 4.10 valence units (*vu*) assuming full occupancy of *Ba*(3) and coordinating anion sites, and 2.92 *vu* when partial occupancies of *Ba*(3) and Cl(2) are taken into account, is much too high. Grice (2001) encountered a similar problem with the crystal structure of fencooperite, $Ba_6Fe^{3+}{}_3[Si_8O_{23}](CO_3)_2Cl_3(H_2O)$, for which he reported bond-valence sums of 1.84, 2.45, 0.87, and 2.45 *vu* to the *Ba*(1), *Ba*(2), *Cl*, and *Fe* sites, respectively. We propose that with respect to kampfite, the bond-valence problems are likely due to (1) the strong hexagonal pseudosymmetry of the structure, and (2) the bond-valence curve for Ba with Cl. We note that the radii (from Shannon 1976) of eight-coordinated Ba and six-coordinated Cl are 1.42 and 1.81 Å, respectively, which results in an ideal Ba–Cl bond distance of 3.23 Å, which is much longer than our Ba(3)–Cl distances of 3.00–3.04 Å. If we use the *R* value from Brese & O'Keeffe (1991) for Ba with Cl (2.69), the bond-valence sum at the Cl atom (coordinated by six Ba atoms) is 1.39 *vu*, which is obviously too high. In order to test the bond-valence curve for Ba with Cl, we found three well-refined, well-ordered crystal structures in the *Inorganic Crystal Structure Database* (2005) in which Cl is coordinated by five Ba atoms at similar distances and in which there are no possible hydrogen bonds to Cl: these are BaClF (Kodama *et al*. 1984), $Ba_5IrIn_2Al_2O_{13}Cl$ (Neubacher & Mueller-Buschbaum

1992), and $Li_2Ba_6H(Si_2O_7)(SiO_4)_2Cl$ (Il'inets *et al.* 1982), and the corresponding bond-valence sums to the Cl atom are 1.06, 1.30, and 1.47 *vu*. Clearly, there is a problem with the bond-valence curve for Ba with Cl, especially for the more complicated compounds, and this is undoubtedly the reason for the high sums for *Ba*(3), Cl(1), and Cl(2).

The atoms at the four *T* sites are all coordinated by four O atoms forming distorted tetrahedra. The *T*(1)–O distances range from 1.636 to 1.667 Å (mean 1.652 Å), and the O–*T*(1)–O angles vary from 104.0 to 112.0° (mean 109.5°). The *T*(2)–O distances range from 1.624 to 1.684 Å (mean 1.662 Å), and the O–*T*(2)–O angles vary from 106.7 to 111.1° (mean 109.5°). The *T*(3)–O distances range from 1.621 to 1.679 Å (mean 1.662 Å), and the O–*T*(3)–O angles vary from 106.9 to 111.1° (mean 109.5°). The *T*(4)–O distances range from 1.628 to 1.665 Å (mean 1.653 Å), and the O–*T*(4)–O angles vary from 103.5 to 112.1° (mean 109.4°). The electron-microprobe data and bond-valence analysis suggest that (Si + Al + Ti) are fully disordered over the four *T* sites.

The atoms at the *C* sites are coordinated by three O atoms to form triangles. The C(1)–O distances are 1.293, 1.308, and 1.320 Å (mean 1.307 Å) and the O–C(1)–O angles are 118.3, 120.5, and 120.7° (mean 119.8°). The C(2)–O distances are 1.291, 1.312, and 1.319 Å (mean 1.307 Å) and the O–C(2)–O angles are 121.7, 119.9, and 117.9° (mean 119.8°). Although the compositional data (admittedly without a direct determination of C concentration) suggest that the *C* sites are filled with C, the refined site-occupancies (1.33) are too high, and those of the coordinating O sites are too low (0.839). As there is no evidence from the compositional data for substitution of other elements at the *C* sites, we suggest that these problems (also) are due to the strong hexagonal pseudosymmetry.

There are 16 distinct anion sites in the kampfite structure (14 O and 2 Cl). The electron-microprobe data and bond-valence analysis suggest that all of the O sites are fully occupied by O, although as noted above, the refined site-occupancy for the O sites coordinating the C sites is low. The electron-microprobe data and refined site-occupancy suggest that the Cl(1) site is fully occupied by Cl, although as noted above, the bond-valence sum [1.69 *vu*, or 1.58 *vu* if the partial occupancy of *Ba*(3) is taken into account] is too high. The Cl(2) site has an occupancy of only 0.240, and is very close to *C*(1) (2.11 Å) and *C*(2) (2.10 Å); we suggest that these problems are also related to the strong hexagonal pseudosymmetry of the structure.

The hexagonal and monoclinic models both have the same number of *Ba*, *T*, and Cl sites. The difference is in the number of *C* positions (one in $P6_3mc$, two in *Cc*) and O (six in the hexagonal model, 14 in the monoclinic model). In the hexagonal model, the C atom is coordinated by three O atoms and the C–O distances are therefore constrained by symmetry to be identical (1.26 Å). As is often the case in crystal structures composed of both heavy and light elements, the heavier atoms define a pseudosymmetry, whereas the true symmetry is revealed by the lighter atoms.

Kampfite is a sheet silicate; the main structural feature is the unbranched single layer $\{\boldsymbol{uB}, 1^2_\infty\}[T_2O_5]$ (Liebau 1985) of six-membered rings, as typical for the mica minerals. In kampfite, however, pairs of polar sheets are joined *via* apical O atoms to form unbranched *zweier* double layers $\{\boldsymbol{uB}, 2^2_\infty\}[T_4O_8]$ (Liebau 1985), oriented parallel to (100) (Figs. 2, 3).

The layers of tetrahedra are connected by three layers of Ba polyhedra. Corner-sharing Ba(1) polyhedra form sheets that are bonded by O(4), O(5), and O(6) atoms to the *T*(3) and *T*(4) tetrahedra, which point along $[\bar{1}00]$ (Fig. 2). Corner-sharing Ba(2) polyhedra form sheets that are connected by O(10), O(11), and O(12) atoms to the *T*(1) and *T*(2) tetrahedra pointing along [100], and Ba(3) polyhedra are located between the sheets of Ba(1) and Ba(2) polyhedra. The CO_3 groups lie between the Ba(1) and Ba(3), and Ba(2) and Ba(3) polyhedra, and are oriented approximately parallel to (100), and the Cl and Ba(3) atoms share planes that are also approximately parallel to (100) (Fig. 2). The layering of $[TO_4]$ tetrahedra and Ba polyhedra is responsible for the perfect {100} cleavage of kampfite.

TABLE 6. BOND-VALENCE* ARRANGEMENT IN KAMPFITE

	Ba(1)	*Ba*(2)	*Ba*(3)	*T*(1)	*T*(2)	*T*(3)	*T*(4)	*C*(1)	*C*(2)	Sum
O(1)	0.25 0.23		0.25						1.31	2.04
O(2)	0.24 0.21		0.27						1.23	1.95
O(3)	0.24 0.22		0.25						1.21	1.92
O(4)	0.17					0.86	0.90			1.93
O(5)	0.17					0.86	0.90			1.93
O(6)	0.08 0.05					0.88	0.92			1.93
O(7)		0.25 0.22	0.25					1.21		1.93
O(8)		0.24 0.22	0.25					1.30		2.01
O(9)		0.24 0.21	0.27					1.25		1.97
O(10)		0.17		0.89	0.89					1.95
O(11)		0.17		0.93	0.85					1.95
O(12)		0.08 0.05		0.92	0.88					1.93
O(13)				0.97			0.99			1.96
O(14)					1.00	1.01				2.01
Cl(1)	0.25	0.25	0.37 0.36 0.37							1.60
Cl(2)			0.10 0.09 0.09							0.28
Sum	2.12	2.10	2.92	3.71	3.62	3.61	3.71	3.76	3.75	

* Calculated from the curves of Brese & O'Keeffe (1991) assuming fully occupied sites except for *Ba*(3) and Cl(2) (see text). Values are expressed in valence units.

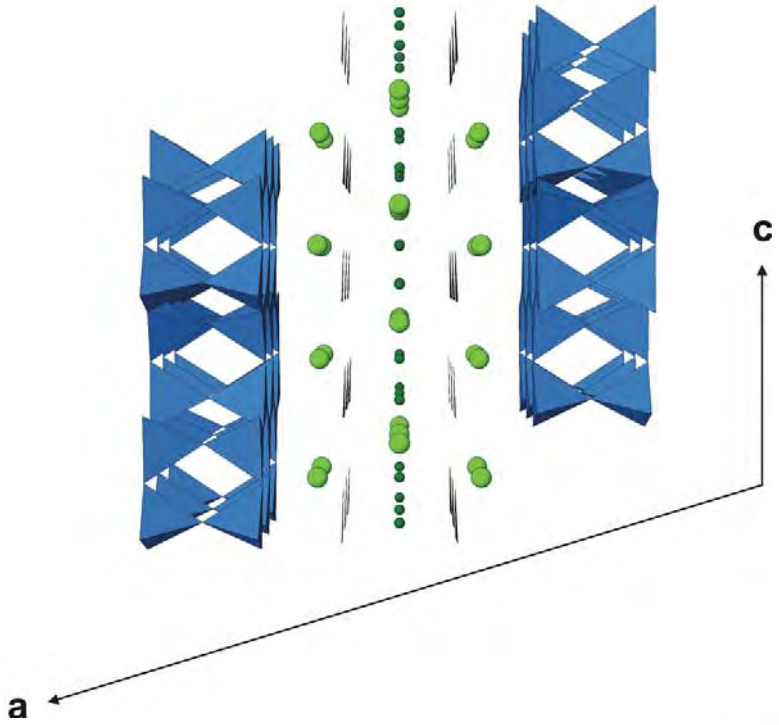

FIG. 2. Perspective drawing (distance 100 Å) of the crystal structure of kampfite projected onto (010). For clarity, only two double layers of tetrahedra and one layer of interstitial atoms are shown. The Ba atoms are shown as light green spheres, [TO_4] tetrahedra are blue, (CO_3) groups are shown as black triangles, and Cl atoms are shown as small dark green spheres.

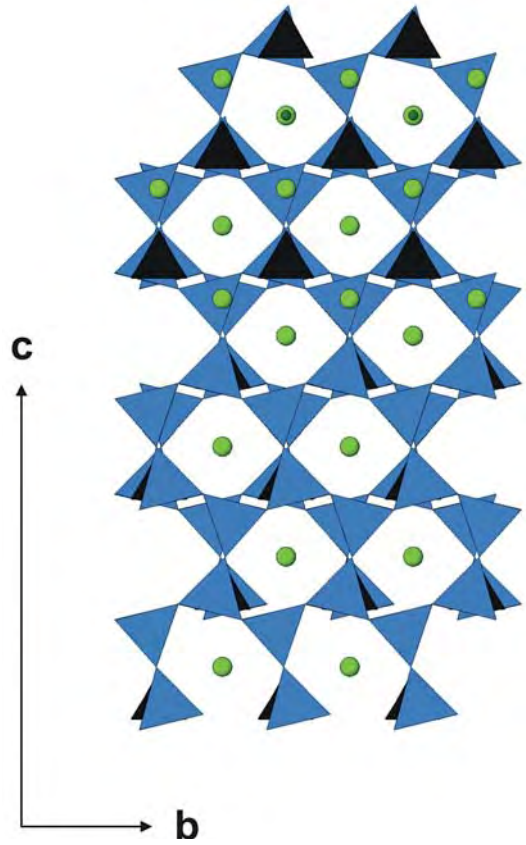

FIG. 3. The crystal structure of kampfite projected onto (100). The same scheme of colors is used as in Figure 2.

Discussion

The ideal formula of kampfite is now considered to be $Ba_{12}(Si_{11}Al_5)O_{31}(CO_3)_8Cl_5$. As stated in Basciano *et al*. (2001), the only other known barium silicate carbonate mineral is fencooperite. The crystal structure of fencooperite also shows layers of (SiO_4) tetrahedra, but these do not form continuous double sheets as found in kampfite, but instead form (Si_8O_{22}) islands of double open-branched triple-branched tetrahedra (Grice 2001).

Grice (2005) compared the 13 described structures of minerals in the silicate–carbonate chemical class. He showed that the degree of polymerization of the silicate tetrahedra increases as the Lewis Base Strength (LBS) decreases from 0.33 *vu* for the nesosilicates to 0.06 *vu* for kampfite, the sole double-sheet silicate. Grice (2005) made the observation that in general, the structures of the silicate–carbonate chemical class are layered with high-coordination polyhedra and carbonate groups in one slab and the silicate groups in another, as seen in the kampfite structure.

The barium minerals of the sanbornite deposits in Fresno County, California, have most recently been described by Walstrom & Leising (2005). At the Rush Creek locality, kampfite occurs with three other barium chloride silicates, traskite, $Ba_9Fe^{2+}{}_2Ti_2(SiO_3)_{12}(OH,Cl,F)_6{\bullet}6H_2O$, titantaramellite, $Ba_4(Ti,Fe^{3+},Fe^{2+},Mg)_4O_2(B_2Si_8O_{27})Cl_x$, where $0 \le x \le 1$, and UKBC–10, a Ba–Fe–Al–Cl silicate related to cerchiaraite (Basso *et al*. 2000). On the basis of a lack of Fe in its formula, kampfite is considered to have formed after these minerals. Inclusions of celsian, witherite, and UKBC–10 have been identified in kampfite from Rush Creek (Basciano *et al*. 2001).

As noted in Basciano *et al*. (2001), kampfite belongs in Dana class 78.1 (unclassified silicates) and is part of VIII/H.38, the monteregianite-(Y) – wickenburgite series [phyllosilicates (layered) mica minerals with double layers of tetrahedra and related structures] in the Strunz system of classification.

The unbranched *zweier* double layers in kampfite have also been described for high-temperature phases of feldspar composition: $Ca[AlSiO_4]_2$ (hT) (Takéuchi & Donnay 1959), $Sr[AlSiO_4]_2$ (hT) and $Pb[AlSiO_4]_2$ (hT) (Pentinghaus 1975), $Ba[AlSiO_4]_2$ (hT) (Takéuchi 1958), and $Rb[AlSi_3O_8]$ (hT) (Sorrel & Negas 1963). They have also been described for the minerals cymrite, $Ba[AlSiO_4]_2{\bullet}H_2O$, vertumnite, $Ca_8Al_4(Al_4Si_5)O_{12}(OH)_{36}{\bullet}10H_2O$, and strätlingite, $Ca_8Al_4(Al_4Si_4)O_8(OH)_{40}{\bullet}10H_2O$.

The crystal structure of cymrite differs from that of kampfite in that there is only one sheet of Ba polyhedra between the double layers of tetrahedra. According to Bolotina *et al*. (1991), the tetrahedra that make up one [T_2O_5] sheet in each double layer are completely filled with Si, and the tetrahedra in the other sheet are completely filled with Al. In order to minimize mismatch between the sheets, the [SiO_4] tetrahedra are rotated about the normal to their bases.

Galli & Passaglia (1978) reported that (like kampfite), vertumnite is metrically monoclinic but strongly pseudohexagonal. The crystal structure consists of modified "brucite-type" layers $^{VII}Ca_2{}^{VI}Al\ (OH,H_2O)_8$ at $z = 0$ and $z = ½$, alternating with double layers of tetrahedra and connected only by hydrogen bonds. The *T* sites are only partly occupied by Si and Al. The H_2O groups are located within the rings of tetrahedra.

Rinaldi *et al*. (1990) showed that the crystal structure of strätlingite contains brucite-type layers made up of ordered ^{VII}Ca and ^{VI}Al polyhedra. The layers are hydrogen-bonded to partially occupied double layers of tetrahedra. The cell dimensions imply stacking of three layers of "octahedra" (as opposed to two in vertumnite) and three double layers of tetrahedra in the [001] direction. Rinaldi *et al*. (1990) claimed that vertumnite and strätlingite are type-II polytypes (mixed-module polytypes with constant proportions of modules) in which the *c* parameter of the former is two-thirds as long as that of the latter. In addition, they used new chemical data for both species to show that strätlingite has a tendency to have a greater proportion of vacant *T*-sites and a higher degree of hydration than in vertumnite.

An obvious difference between the crystal structure of kampfite and those of the three minerals described above is the composition of the unbranched *zweier* double layers. In cymrite, vertumnite, and strätlingite, the Al:Si ratio is 1:1 (cymrite and strätlingite) or close to it (vertumnite), whereas in kampfite the Al:Si ratio is 5:11. It is also interesting to note that vertumnite and strätlingite have vacancies at the *T* sites. The presence of vacancies, the pseudosymmetry displayed by kampfite and vertumnite, and the relative rarity of minerals with unbranched *zweier* double layers all suggest that there are significant geometrical constraints to the formation of crystal structures with this feature.

Acknowledgements

We thank R. Rowe for collecting the powder-diffraction data and M.A. Cooper for help with the data collection and refinement. The manuscript was improved by comments from R.A. Gault, J.D. Grice, Yu. Uvarova, an anonymous reviewer, D.T. Griffen, and R.F. Martin. Financial support was provided by the Natural Sciences and Engineering Research Council of Canada in the form of a Discovery grant to LAG and Major Facility Access and Major Equipment grants to F.C. Hawthorne.

References

Basciano, L.C., Groat, L.A., Roberts, A.C., Grice, J.D., Dunning, G.E., Foord, E.E., Kjarsgaard, I.M. & Walstrom, R.E. (2001): Kampfite, a new barium silicate

carbonate mineral species from Fresno County, California. *Can. Mineral.* **39**, 1053-1058.

Basso, R., Lucchetti, G., Zefiro, L. & Palenzona, A. (2000): Cerchiaraite, a new natural Ba–Mn-mixed-anion silicate chloride from the Cerchiara mine, northern Apennines, Italy. *Neues Jahrb. Mineral., Monatsh.*, 373-384.

Bolotina, N.B., Rastsvetaeva, R.K., Andrianov, V.I. & Kashaev, A.A. (1991): Refinement of modulated crystals: structure of cymrite. *Sov. Phys. Crystallogr.* **36**, 190-194.

Brese, N.E. & O'Keeffe, M. (1991): Bond-valence parameters for solids. *Acta Crystallogr.* **B47**, 192-197.

Galli, E. & Passaglia, E. (1978): Vertumnite: its crystal structure and relationship with neutral and synthetic phases. *Tschermaks Mineral. Petrogr. Mitt.* **25**, 33-46.

Grice, J.D. (2001): The fencooperite crystal structure: unique [$Fe^{3+}O_{13}$] pinwheels cross-linked by [Si_8O_{22}] islands. *Can. Mineral.* **39**, 1065-1071.

Grice, J.D. (2005): The structure of spurrite, tilleyite, and scawtite, and relationships to other silicate–carbonate minerals. *Can. Mineral.* **43**, 1489-1500.

Il'inets, A.M., Ilyukhin, V.V., Belov, N.V. & Nevskii, N.N. (1982): The crystal structure of barium chlorosilicate. *Dokl. Akad. Nauk SSSR* **267**, 1125-1127.

Inorganic Crystal Structure Database (2005): Fachinformationszentrum Karlsruhe, Germany.

International Tables for X-Ray Crystallography (1992): Vol. C. Kluwer Academic Publishers, Dordrecht, The Netherlands.

Kodama, N., Tanaka, K., Utsunomiya, T., Hoshino, Y., Marumo, F., Ishizawa, N. & Kato, M. (1984): An X-ray diffraction study of anharmonic thermal vibrations in the ionic conductor, barium chloride fluoride BaClF. *Solid State Ionics* **14**, 17-24.

Le Page, Y. (1987): Computer derivation of the symmetry elements implied in a structure description. *J. Appl. Crystallogr.* **20**, 264-269.

Liebau, F. (1985): *Structural Chemistry of Silicates: Structure, Bonding, and Classification*. Springer-Verlag, New York, N.Y.

Mandarino, J.A. (1981): The Gladstone–Dale relationship. IV. The compatibility concept and its application. *Can. Mineral.* **19**, 441-450.

Neubacher, M. & Mueller-Buschbaum, H. (1992): Ein neues Erdalkalimetall-Chlorooxometallat mit Ir^{5+}: $Ba_5Ir In_2Al_2O_{13}Cl$. *J. Alloys Compounds* **183**, 18-23.

Pentinghaus, H. (1975): Hexacelsiane. *Fortschr. Mineral.* **53**, 1-65.

Rinaldi, R., Sacerdoti, M. & Passaglia, E. (1990): Strätlingite: crystal structure, chemistry, and a reexamination of its polytype vertumnite. *Eur. J. Mineral.* **2**, 841-849.

Shannon, R.D. (1976): Revised effective ionic radii and systematic studies of interatomic distances in halides and chalcogenides. *Acta Crystallogr.* **A32**, 751-767.

Sorrel, C.A. & Negas, T. (1963): Metastable rubidium aluminium silicate with a hexagonal sheet structure. *Science* **141**, 917.

Takéuchi, Y. (1958): A detailed investigation of the structure of hexagonal $BaAl_2Si_2O_8$ with reference to its α–β inversion. *Mineral. J.* **2**, 311-332.

Takéuchi, Y. & Donnay, G. (1959): The crystal structure of hexagonal $CaAl_2Si_2O_8$. *Acta Crystallogr.* **12**, 465-470.

Walstrom, R.E. & Leising, J.F. (2005): Barium minerals of the sanbornite deposits, Fresno County, California. *Axis* **1**, 1-18.

Received September 14, 2006, revised manuscript accepted January 10, 2007.